Diagenesis of the Permian Fengcheng Formation Shale Series in the Mahu Sag, Junggar Basin, China

Bin Bai *, Jiwei Liang, Chaocheng Dai, Wenjun He, Zhenkun Yu, Ying Bai, Xiaobin Chang, Meng Zheng, Hanlin Li, Hao Zong

Posted Date: 20 October 2023

doi: 10.20944/preprints202310.1320.v1

Keywords: alkaline diagenesis; shale series; Fengcheng Formation; Mahu Depression; Junggar Basin; China

Article

Diagenesis of the Permian Fengcheng Formation shale series in the Mahu Sag, Junggar Basin, China

Bin Bai [1,*], Jiwei Liang [2], Chaocheng Dai [3], Wenjun He [4], Zhenkun Yu [5], Ying Bai [1], Xiaobin Chang [2] , Meng Zheng [2], Hanlin Li [2] and Hao Zong [2]

[1] Research Institute of Petroleum Exploration & Development, PetroChina, Beijing 100083, China
[2] School of Earth Sciences and Resources, Chang'an University, Xi'an 710054, China
[3] School of Earth Sciences, East China University of Technology, Nanchang 330013, China
[4] Research Institute of Exploration and Development，Xinjiang Oilfield Company，PetroChina, Karamay, Xinjiang 834000, China
[5] Shandong Provincial NO.4 Institute Of Geological and Mineral Survey,Wei'fang 261021,China.
* Correspondence: baibin81@petrochina.com.cn

Abstract: The Fengcheng Formation in the Mahu Sag of the Junggar Basin was generally composed of detritus, pyroclastic material, carbonates, and evaporites. During the process of sedimentation, the climate was arid or semi-arid. Due to the effect of high concentration and sodium-rich source, an alkaline lake was formed, and alkaline minerals were also preserved in the stratum. After the sediments were buried, three mineral assemblages were formed in the Fengcheng Formation, which are carbonate mineral assemblages (i.e., calcite + ferreous dolomite), reedmergnerite and carbonate mineral assemblages (i.e., reedmergnerite + calcite + ferreous dolomite), and reedmergnerite and alkaline mineral assemblages (i.e., reedmergnerite + shortite + trona), respectively. According to the homogenization temperature of reedmergnerite primary fluid inclusions, alkaline diagenesis of Fengcheng Formation is divided into early stage（≤100℃） and middle stage（＞100℃）, respectively. The former is characterized by the generation of ferreous saddle dolomite, quartz dissolution, and agglutination of the laumontite, which occurred under normal burial conditions. The latter is marked by the reedmergnerite's appearance, which is correlated to deep hydrothermal activity controlled by faults. Finally, based on sedimentary and diagenetic factors, including climate, provenance, diagenetic surroundings, and the action of subsurface fluid, the alkaline deposition-diagenesis model for shale series in four stages of the Fengcheng Formation was established.

Keywords: alkaline diagenesis; shale series; Fengcheng Formation; Mahu Depression; Junggar Basin; China

1. Introduction

Traditional early and middle diagenesis is mainly conducted in acidic diagenetic environment, which is characterized by that carbonate mineral, feldspar, and clay minerals are in an unstable state and easy to be dissolved [1-5]. When the reservoir experienced an alkaline diagenetic environment, reservoir property reservoir property is often changed due to the role of alkaline formation water, quartz dissolution, feldspar enlargement, and carbonate mineral replacement become the most distinctive diagenetic phenomena [6-11]. The theory of alkaline diagenesis has enriched, improved and deepened the traditional theory of diagenesis. At present, the understanding of alkaline diagenesis is relatively insufficient compared with traditional diagenesis. The conditions of alkaline diagenesis generally include sedimentary environment, climate, organic acids and thermal fluid evolution [12-13]. Alkaline diagenesis can have constructive effects on reservoirs [14-15]. For example, mica interlaminar pores and albite pores formed under the action of alkaline fluids are good oil storage spaces. The diagenetic phenomena of alkaline diagenesis are diverse, including alkali lacustrine salt rocks [16], alkaline evaporative salt minerals [17], and quartz dissolution under the action of alkaline groundwater [18]. In addition, alkaline diagenesis may also provide a new

 doi:10.20944/preprints202310.1320.v1

explanation for the silicification of metal deposits, the origin of siliceous cementation, and the reddening and fragmentation of rocks [11-19].

Fengcheng Formation in Mahu Sag, northwestern Junggar Basin, is a set of mixed shale series composed of carbonate rocks, alkaline intermediate-basic volcanic rocks and terrigenous detrital rocks, containing alkaline minerals such as kanemite, bradleyite, and eitelite, which may have been formed in alkaline lake environment [20]. The rocks also contain bands and clumps of the uncommon mineral reedmergnerite [$Na(BSi_3O_8)$], indicating that it has undergone complex diagenetic processes [4-6]. Fengcheng Formation is a fair to good source rock development horizon with high organic matter content [20-21]. It has the characteristics of multi-phase hydrocarbon generation peak and large-area hydrocarbon generation. It has good exploration prospects and development value and has been widely concerned recently. Studies show that the alkali lake of Fengcheng Formation has experienced five stages of drought-wet-dry-heat-continuous dry-heat-humid [22], forming major reservoir types including dolomite, clastic rock, and volcanic rock, and the formation of alkaline minerals is closely related to the evaporative salinization of lake brine [23]. The study of the alkaline lake environment and its diagenesis is still in the initial stage and needs to be further studied. The petrological characteristics, mineralogical characteristics, diagenetic types, and sedimentary-diagenetic models of Fengcheng Formation in Junggar Basin were studied using electron probe, scanning electron microscope, cathode luminescence, and laser Raman in order to be helpful for shale oil and gas exploration and development.

2. Geological Setting and Samples

The Junggar Basin is located in northwestern China (Figure 1a), with an area of about 1393 square kilometers [24]. The northeast of the basin is close to the Qingridi Mountains and Kelamei Mountains, the south is adjacent to the Tianshan Mountains, and the northwest-west are the Delun Mountains, Halaalate Mountains, and Zaire Mountains, which are nearly triangular with a sharp southeast and a wide northwest (Figure 1a). The Junggar Basin is an important part of the Central Asian Orogenic Belt [25-26]. The basin is divided into six first-level structural units: Ulungu Sag, Luliang Uplift, Western Uplift, Central Sag, Eastern Uplift, and North Tianshan Thrust Band [25] (Figure 1a). The Junggar Basin belongs to the superimposed basin [27-28], whose Late Devonian-Early Carboniferous were rift basins, while the Late Carboniferous-Permian formed foreland basins, and the Triassic-Paleogene were intracontinental depression basins [29]. From the Early Paleozoic to the end of the Late Paleozoic Carboniferous, the Junggar Basin had a long-term multi-island oceanic paleogeographic pattern with discrete island arcs and ocean basins arranged alternately [26, 30], and with the evolution of the Paleo-Asian Ocean Basin, the marine area gradually diminished [26]. When the Jiamuhe Formation was deposited in the Early Permian, some areas in the basin evolved into residual marine facies [41], until the Early Permian Fengcheng Formation. During this period, the Fengcheng, Wuerhe, and Xiazijie areas in the Mahu sag evolved into salinized lake basin facies after the closure of the residual sea [22].

The Mahu sag is located in northwest of the central sag of the Junggar Basin in an NE trend. It is a secondary structural unit in the basin [27], with a length of about 100 km, a width of about 50 km, and an area of about 5 000 square kilometers [33]. The tectonic unit dips gently to the southeast as a whole [34], and is one of the sags with the richest oil and gas content in the basin [35, 36]. The Mahu sag is adjacent to the Kebai and Wuxia large fault zones in the northwest [37], the Yingxi sag in the east, the Dabasong-Xiayan uplift in the southeast, and the Zhongguai uplift in the southwest [22, 38] (Figure 1a), developed on the pre-Carboniferous folded basement [29]. The Lower Permian Fengcheng Formation is the main source of rock formation in the Mahu Sag [39], with a maximum formation thickness of 1500 m [23]. It is the oldest alkali lacustrine source rock discovered in the world so far [40], experienced three periods of hydrocarbon generation peaks: Late Permian, Late Triassic, and Late Cretaceous [28], and the generated oil and gas were accumulated in the Fengcheng Formation and its overlying Wuerhe Formation and Baikouquan Formation [40]. According to the rock combination, from bottom to top, the Fengcheng Formation can be divided into three sections, including Feng 1, Feng 2, and Feng 3. The Feng1 Member mainly develops volcanic rocks, the Feng

Preprints (www.preprints.org) | NOT PEER-REVIEWED | Posted: 20 October 2023 doi:10.20944/preprints202310.1320.v1

2 Member develops mudstone and carbonate rocks, which are rich in reedmergnerite, and the Feng
3 Member mainly develops terrigenous detrital rocks (Figures 1b-c).

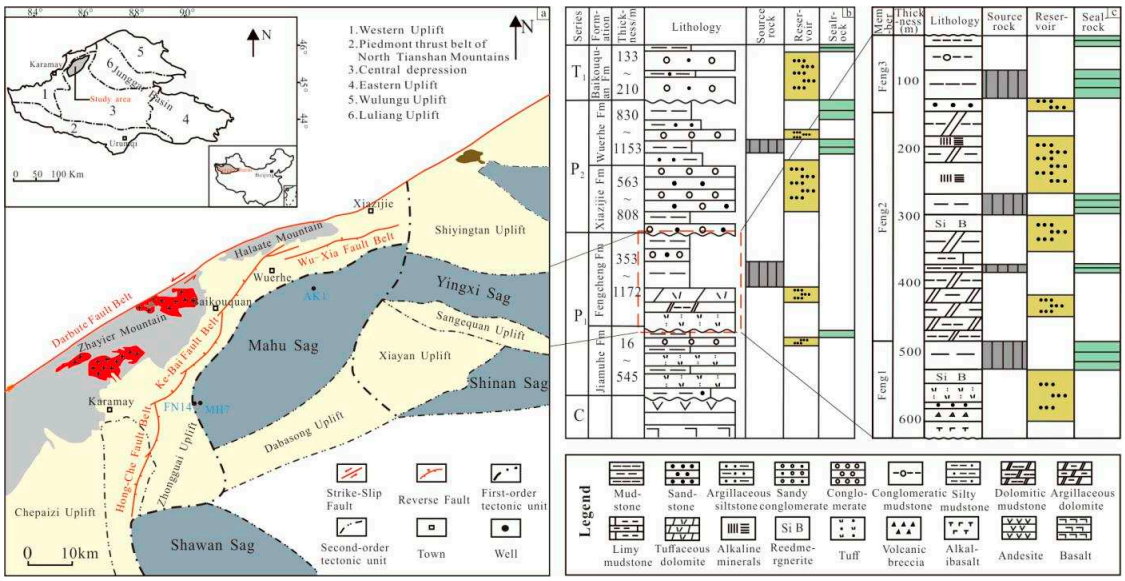

Figure 1. Tectonic and lithofacies paleogeographic maps of Mahu Depression, Junggar Basin: (**a**) Map of tectonic units in Mahu Depression, Junggar Basin (with well location) (adapted from [14, 28]); (**b**) Lithologic columns of Permian and Fengcheng Formation in Mahu Depression (adapted from [26]); (**c**) Source-reservoir-cap assemblage diagram (taking well FN1 as an example).

3. Analytical Methods

Castings and multi-purpose slices of exploratory well cores such as FN1, FN14, AK-1, and MH7 are used as the main experimental objects. Firstly, the multi-purpose and cast thin sections were analyzed by polarized light microscope to obtain key information such as the type, morphology and mutual relationship between minerals in thin sections, and the pores were observed. At the same time, the microscopic features of minerals such as quartz, zeolite and clay were recorded under the scanning electron microscope (SEM), and the ring-band structure of carbonate minerals was observed in the cathode luminescence (CL) test. The scanning electron microscope (SEM-QUANTA650) experiment was completed in the Mineralization and Dynamics Laboratory of Chang'an University, and the cathode luminescence (CL 8200mk5-2) test was carried out in the Xi'an National Engineering Laboratory for Low Permeability Oil and Gas Field Exploration and Development. For Mg-Ca carbonate minerals and special alkaline minerals widely distributed in thin slices, electron probe microanalysis (EPMA) is used to determine the composition of carbonate minerals and the specific content of each component, and to assist in determining the type of alkaline minerals. Because the reedmergnerite in alkaline minerals is special, the laser Raman method (LR) was used to analyze it. The LinkamTHMS600 geological cold and hot platform was used for testing homogenization temperature of reedmergnerite primary fluid inclusions. The electron probe (EPMA-JXA8100) experiment was completed in the Mineralization and Dynamics Laboratory of Chang'an University, and the laser Raman (Renishaw inVia type confocal laser Raman spectrometer) test experiment was completed in the Xi'an Institute of Geology and Mineral Resources. In order to avoid the interference of external substances and assure the accuracy of the experimental results, all core slices are stored in slice boxes before the experiment, and the experimental process is strictly operated according to the standard [4-8].

 doi:10.20944/preprints202310.1320.v1

4. Results

4.1. Petrological characteristics

Fengcheng Formation is a set of mixed shale series composed of alkaline intermediate-basic volcanic rocks, carbonate rocks and terrigenous clastic rocks (Figures 1b-c).

Volcanic rocks are one of the rock types in the study area, which are mainly developed in the Fengcheng1 Member, and can be divided into three categories: shallow intrusive rocks, volcanic lava and volcanic clastic rocks. Shallow intrusive rocks are also divided into basaltic porphyrite and esitic porphyrite. Volcanic lava can be subdivided into basalt, andesitic rock and trachyte. Volcanic clastic rocks include tuff and breccia. There are more tuff and basalt. Rock and mineral identification and previous studies show that the volcanic rocks are mainly intermediate-basic. The discovery of the silica-alkali diagram and titan pyroxene (Table 1) of volcanic rocks shows that the volcanic rocks of the Fengcheng Formation are alkaline.

Table 1. EPMA data table of titanaugite (at. %).

Na_2O	TiO_2	SO_3	SiO_2	FeO	P_2O_5	Al_2O_3	MnO	K_2O	MgO	BaO	CaO
0.024	20.276	0.056	37.513	8.687	0.051	6.745	0.122	0.116	2.243	0.073	18.156

Cabonate rocks are mainly dolostone and argillaceous dolomite, developed in the second member of the Fengcheng Formation, while only thin or small cabonate lenses are found in the Fengcheng 1 Member and the Fengcheng 3 Member. The middle striation of dolomite is developed, and most interbedded with argillaceous rocks. Dolomite are mostly fine-grained with microcrystalline clays and the content of dolomite is 45-65 at.% (atomic percent). A small amount of volcanic tuff, including volcanic eruptions and terrigenous, fine-grained tuff debris, is visible in some dolomites [43].

The terrigenous clastic rocks are conglomerate, sandstone, and mudstone. The conglomerate and sandstone are developed in the Fengcheng 3 Member. Dolomite particles and volcanic tuff are common in the rocks. The closer the lake basin edge is, the larger the particle size is, and the debris may mainly come from the Zaire Mountain in the west of the Mahu Sag [44-45]. Mudstone is very common in Feng 1, Feng 2, and Feng 3 sections. The thickness of Feng 2 is large, and it is rich in bacteria and algae organic matter [22-24]. It is the main source rock position of the Fengcheng Formation. There are seasonal laminae [44-46]. Microcrystalline calcite in some areas of mudstone experienced dolomitization and transformed to dolomite with the lake water as the Mg source.

4.2. Mineralogical characteristics

Fe-bearing dolomite, calcite, and so on are important diagenetic mineral components of the Fengcheng Formation shale series in Mahu Sag. Studying the relationship between them is of great significance for the classification of alkaline diagenesis. The Fengcheng Formation in this area is preliminarily divided into three mineral assemblages: carbonate mineral assemblage, borosilicate-carbonate mineral assemblage, and borosilicate-alkaline mineral assemblage.

The dolomite of the Fengcheng Formation is generally iron-containing (Table 2), with the highest iron content of 13 % and an average of 8.5% [47]. Fe^{2+} does not replace half of Mg^{2+}, so it is iron dolomite. There are three forms of iron dolomite: mud microcrystal layered (Figure 2a), powder crystal block (Figures 2b-c), and snowflake (Figures 2d-e). Under cathode luminescence, the band structure of mud-microcrystalline layered iron dolomite is only occasionally seen. The fine-grained block and snowflake-like iron dolomite have a clear ring structure, which can be divided into irregular undulate type I ring combination (Figure 2e) and rhombic type II ring combination (Figure 2f). The edge morphology of the outermost ring of the type II ring combination is different, mostly in a straight shape (Figure 2f), and occasionally in a serrated or clamshell shape, which may be caused by late corrosion events [38-39]. It is difficult to see pure calcite in Fengcheng Formation. Calcite has been replaced by dolomite or iron dolomite, and a small part has been replaced by sodium

 doi:10.20944/preprints202310.1320.v1

borosilicate (Figure 2g). Reedmergnerite [$Na(BSi_3O_8)$] is a rare diagenetic mineral, mainly distributed in the Feng1 and Feng 2 Member and often coexists with carbonate minerals. After calcite dolomitization, iron dolomite was replaced by borosilicate, some reedmergnerite developed metasomatic relict texture, and carbonate minerals remained in the minerals (Figures 2h-i). It is inferred that the formation age of borosilicate is later than that of carbonate minerals. The reedmergnerite can be divided into two types according to the degree of self-shape: wedge-shaped reedmergnerite with a high degree of self-shape and diamond-plate-shaped reedmergnerite with a low degree of self-shape (Figure 3b) and wreck-shaped reedmergnerite (Figure 2h). The former is mostly aggregated growth (Figure 3a), while the latter is mostly scattered in the matrix. The mineral is not pure inside, and the mineral edge is jagged or irregularly radial.

Under the microscope, the butterfly-shaped twinned crystals and a group of complete cleavages can be seen in the high degree of self-shaped reedmergnerite. Under the cathodoluminescence, reedmergnerite emits blue light with different intensities (Figure 3c). Since boron element is located at the lowest detection ability of electron probe microanalyzer (EPMA) [50], the total content of each component in reedmergnerite measured in this paper is about 79-85 %, less than 100 % (Table 3). The difference may be that the content of B_2O_5, and the content of B_2O_5 after treatment is close to the standard content of B_2O_5 in reedmergnerite [51]. In order to enhance credibility and accuracy, the laser Raman (LR) method was used to test the reedmergnerite. The test spectra showed that the transverse coordinates of the four characteristic peaks were 230 cm^{-1}, 600 cm^{-1}, 1000 cm^{-1}, and 1600 cm^{-1}, respectively. The transverse coordinates of the main peak were 600 cm^{-1}, which was similar to the characteristics of the Reedmergnerite Raman spectra [52] (Figure 4).

Reedmergnerite often appears with alkaline minerals. Due to the limitation of the number of drilling wells, it was found in the samples of the Fengcheng Formation that wollastonite was mainly symbiotic with trona and shortite (Figures 3d-e). From the metasomatism relationship between them, for example, reedmergnerite starts to replace the shortite from the edge (Figure 3d), it can be seen that the formation of reedmergnerite is later than alkaline minerals.

Table 2. EPMA data table of iron dolomite (at.%).

Na_2O	TiO_2	SO_3	SiO_2	FeO	P_2O_5	Al_2O_3	MnO	K_2O	MgO	BaO	CaO
0.07	0.22	-	-	9.39	-	0.01	0.46	0.01	15.49	0.09	27.91
-	-	-	0.03	9.38	0.06	0.02	0.62	0.02	15.01	-	27.85
-	-	0.06	-	8.01	-	-	0.11	0.01	17.58	-	30.84
-	-	-	-	6.44	0.02	0.02	0.37	-	17.99	0.09	32.02
-	0.04	0.04	0.01	12.99	-	0.05	0.33	-	13.96	-	29.45
-	-	0.04	-	10.98	0.04	0.01	0.54	0.01	13.74	0.07	28.03
-	-	-	0.16	6.69	-	0.08	0.18	0.03	17.85	0.04	31.10
-	-	0.04	-	8.41	0.01	-	1.21	0.04	18.25	-	32.05
-	0.05	-	-	7.45	0.01	-	0.86	-	17.49	0.13	30.46
0.07	0.08	0.25	8.54	5.43	0.08	1.86	0.16	0.54	15.58	-	23.58

Preprints (www.preprints.org) | NOT PEER-REVIEWED | Posted: 20 October 2023 doi:10.20944/preprints202310.1320.v1

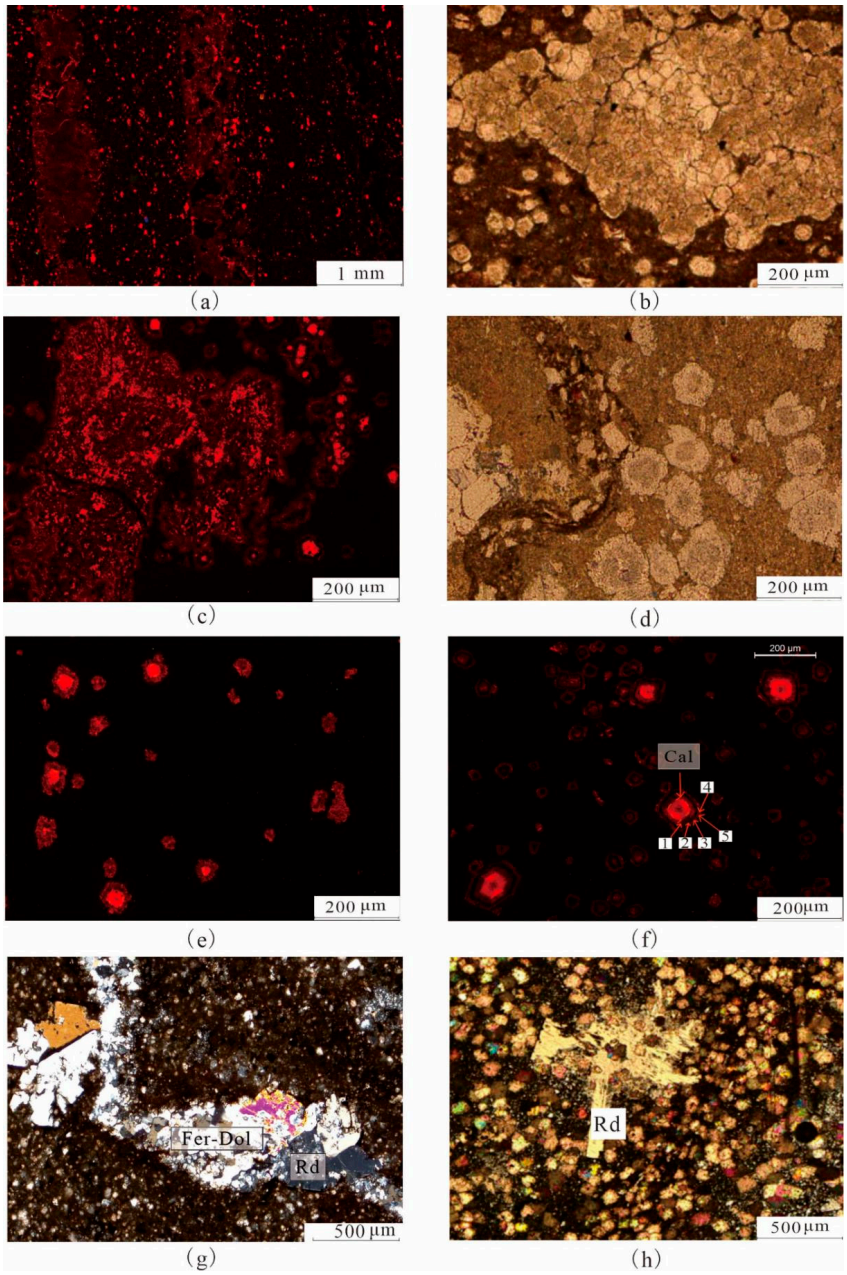

Figure 2. Petrological characteristics in Mahu Depression, Junggar Basin: (**a**) MY1-F2, Characteristics of lamellar iron dolomite under cathodoluminescence; (**b-c**) FN14-F2, Microscopic characteristics of massive iron dolomite and its cathodoluminescence properties; (**d-e**) FN14-F2, Microscopic characteristics of snowflake iron dolomite and its cathodoluminescence properties; (**f**) FN14-F2, Bright iron-poor nuclei (Cal), the number of bands indicated by 1,2,3; (**g**) FN14-F2, The calcite (Cal) in the belt is metasomatized almost entirely by ferric dolomite (Fer-DOL), which is metasomatized later by reedmergnerite (Rd); (**h**) FN14-F2, Skeletal crystalline reedmergnerite with irregular radial edges.

Table 3. EPMA data table of reedmergnerite (at.%).

Na_2O	TiO_2	SO_3	SiO_2	FeO	P_2O_5	Al_2O_3	MnO	K_2O	MgO	BaO	CaO	B_2O_5
10.000	-	-	70.517	-	-	-	-	0.001	0.010	0.025	-	19.447
10.000	-	0.010	69.767	0.028	-		0.043	0.012		-	-	20.118
13.794	-	-	71.165	0.009	0.025	0.047	-	-	0.007	-	0.005	14.948
11.936	0.065	-	69.377	0.017	0.017	0.068	-	0.062	0.014	0.016	0.013	18.415
10.012	-	0.162	69.697	0.020	0.017	0.086	-	0.088	0.027	-	-	19.891

Preprints (www.preprints.org) | NOT PEER-REVIEWED | Posted: 20 October 2023 doi:10.20944/preprints202310.1320.v1

10.000	0.258	-	70.632	-	-	0.094	0.009	0.008	0.028	0.007	-	18.964
10.063	0.080	0.031	70.288	-	-	0.010	-	0.015	-	-	-	19.513
10.042	-	0.005	70.015	0.004	-	0.003	0.025	0.024	-	-	0.004	19.878
10.072	0.032	-	64.868	0.009	0.017	0.004	0.024	0.021	0.018	-	-	20.935

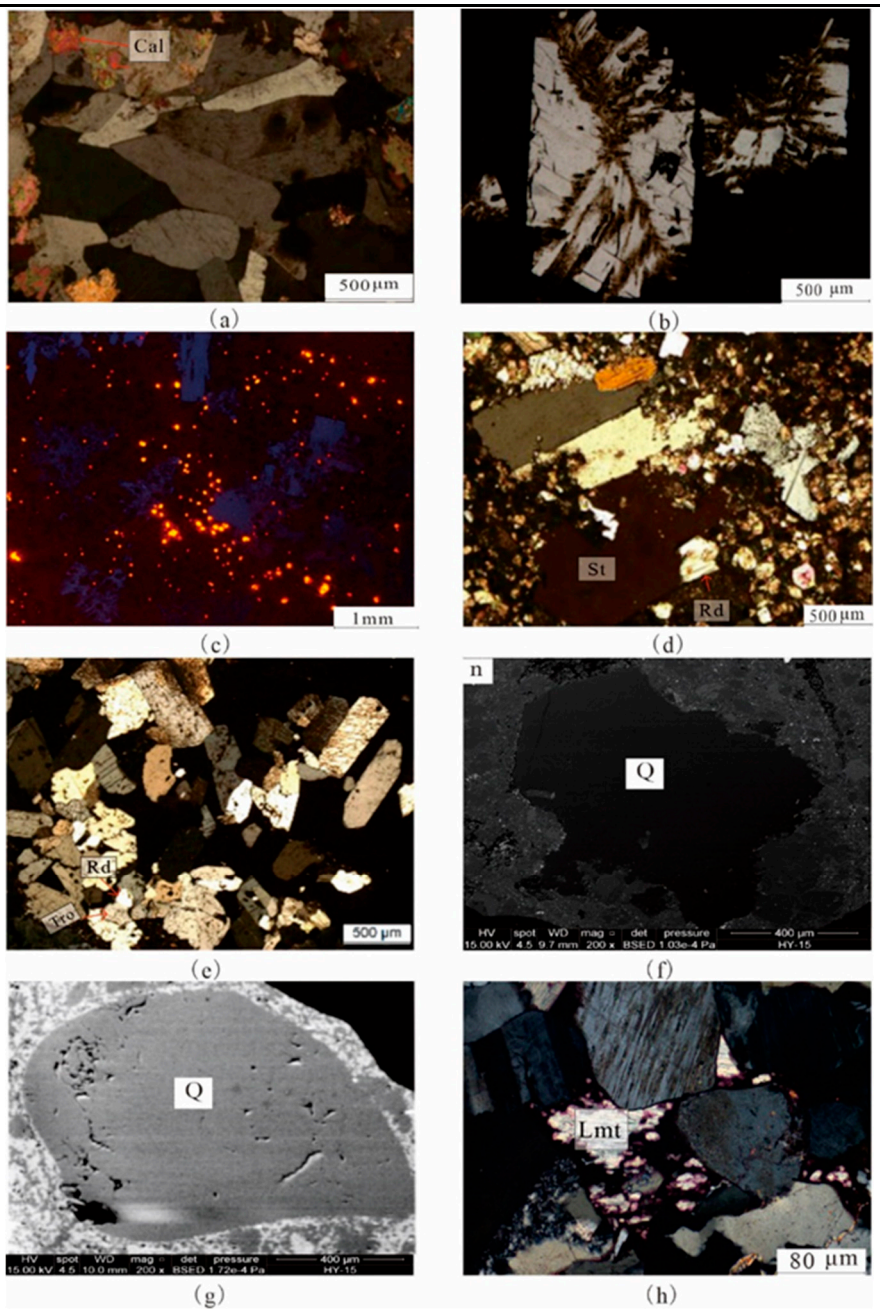

Figure 3. Alkaline diagenesis characteristics in Mahu Depression, Junggar Basin: (**a**) FN14-F2, Wedge-shaped reedmergnerite are clustered together, and some of them contain residual calcite (Cal).; (**b**) FN14-F2, Rhomboid reedmergnerite with serrated edges; (**c**) FN14-F2, Under cathodoluminescence, the reedmergnerite shows dark blue; (**d**) FN14-F2, Reedmergnerite (Rd) metasomatism of shortite (St) from the edge; (**e**) AK1-F2, Reedmergnerite (Rd) is symbiotic with trona (Tro); (**f**) FN14-F1, The edge of quartz grain is corroded into serrated or bay shape; (**g**) MY1-F1, the internal surface of quartz was dissolved to form a "honeycomb" pit, 200 times; (**h**) MY1-F1, Laumonite cemented between particles (Lmt).

Preprints (www.preprints.org) | NOT PEER-REVIEWED | Posted: 20 October 2023 doi:10.20944/preprints202310.1320.v1

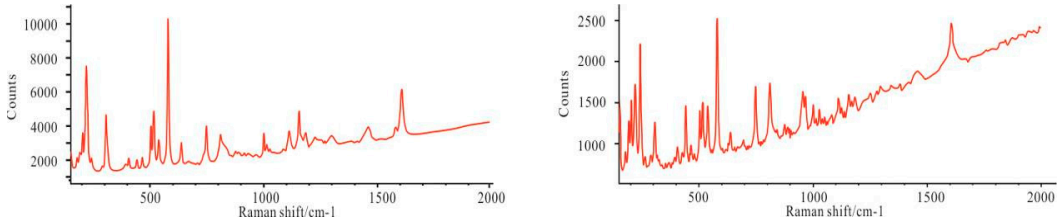

Figure 4. Laser raman spectroscopy of reedmergnerite.

4.3. Homogenization temperature of reedmergnerite primary fluid inclusions

According to the phase combination and microscopic fluorescence characteristics of fluid inclusions at room temperature, the fluid inclusions of reedmergnerite can be divided into five categories: (1) Liquid only inclusions (L-O) in a single liquid phase without visible bubbles. (2) Liquid dominated two-phase inclusions (L-D) with a gas-liquid ratio less than 50%. (3) Single liquid phase oil inclusions emitting blue light under fluorescence. (4) Gas-liquid two-phase oil inclusions with a gas-liquid ratio of less than 50% emitting blue light under fluorescence. (5) Oil inclusions emitting yellow light under fluorescence. The occurrence of fluid inclusions mainly includes four types: (1) The inclusions in the growth zone(GZ) often exhibit mineral growth characteristics (Figure 5a, b), and these inclusions are considered reliable primary inclusions. fluid inclusions within the same growth zone belong to the same associations of fluid inclusions(FIA). (2) Clustered inclusions (Figure 5c) are usually clustered in a relatively small area, and clustered inclusions may be primary or secondary. When they are primary inclusions, they belong to the same FIA. (3) Random population (RP) inclusions, which are randomly and directionally distributed in a relatively large area (Figure 5d), are of unknown origin and may be either primary or secondary. In any case, such inclusions do not belong to the same FIA. (4) The inclusion in Long Trail (LT) refers to a healing crack that cuts through the mineral boundary (Figure 5e, f), the inclusion produced as a healing crack is considered a typical secondary inclusion, and the inclusion produced in the same healing crack belongs to one FIA[53].

Through systematic analysis of fluid inclusion petrography, the inclusions in the study area mainly exhibit the following five types of associations: (1) Rich liquid two-phase saline inclusions with relatively consistent gas-liquid ratios were detected in the growth zone of reedmergnerite minerals (Figure 5b). (2) A rich liquid phase two-phase brine inclusion was detected in the long healing crack of cut borosilicate (Figure 5f). (3) The long healing crack of cut borosilicate was detected as a rich liquid phase two-phase oil inclusion with green fluorescence (Figure 5g, h). (4) Rich liquid phase two-phase oil inclusions with yellow and blue fluorescence were detected in multiple long healing cracks of cut borosilicate (Figure 5i). (5) Long healing cracks in cut borosilicate have been detected, with yellow fluorescent two-phase oil inclusions in the rich liquid phase and two-phase saline inclusions in the rich liquid phase.

A total of 15 L-D fluid inclusions with relatively consistent gas-liquid ratios were detected in the growth band, forming 3 FIAs. The 3 FIAs showed consistent temperature measurement data (Table 4), and the homogenization temperature (Th) range of 15 L-D fluid inclusions was 100℃-116℃ (Figure 6).

Preprints (www.preprints.org) | NOT PEER-REVIEWED | Posted: 20 October 2023 doi:10.20944/preprints202310.1320.v1

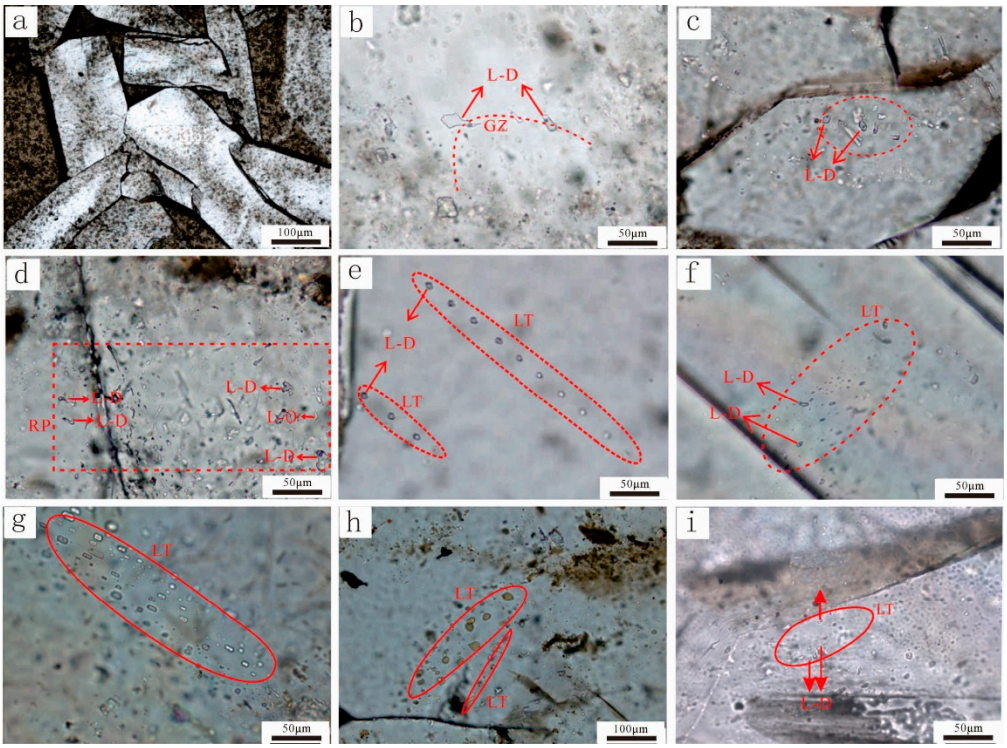

Figure 5. Fluid characteristics of the fluid inclusion in reedmergnerite.

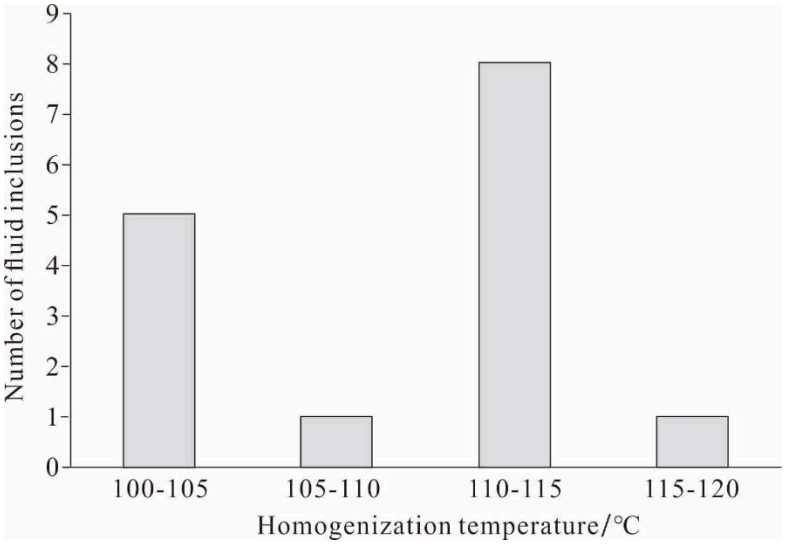

Figure 6. Homogenization temperature histogram of reedmergnerite primary fluid inclusions.

Table 4. Results of homogenization temperature of the fluid inclusion in reedmergnerite.

Borehole	Deep/m	Fluid inclusions occurrence	Associations of fluid inclusions	Type	Size/μm	Homogenization temperature/°C
Fengnan2	4100.58	growth zone	FIA-1	gas & liquid	20	112
				liquid	10	100
				liquid	15	111
Fengnan2	4100.58	growth zone	FIA-2	gas & liquid	5	112
				gas & liquid	4	100
				liquid	4	111

Preprints (www.preprints.org) | NOT PEER-REVIEWED | Posted: 20 October 2023 doi:10.20944/preprints202310.1320.v1

				liquid	5	112
				liquid	4	100
Fengnan2	4100.58	growth zone	FIA-3	gas & liquid	4	111
				gas & liquid	6	104
				gas & liquid	5	103
				liquid	7	109
				liquid	5	110
				liquid	7	116
				liquid	6	112

5. Discussion

5.1. Types of alkaline lake diagenesis and their causes

The diagenetic minerals such as iron dolomite and laumontite can be formed under normal burial temperature conditions. However, the temperature of reedmergnerite formation is relatively high[54-55]. According to the homogenization temperature of reedmergnerite primary fluid inclusions, alkaline diagenesis of Fengcheng Formation is divided into two stage, that is early stage （≤100℃） and middle stage（＞100）, early stage corresponding low-temperature alkaline diagenesis, and middle stage corresponding medium-high-temperature alkaline diagenesis. The manifestations of low-temperature alkaline diagenesis include the formation of iron dolomite rings, quartz dissolution and cementation of laumontite, and the appearance of reedmergnerite marks the medium-high temperature alkaline diagenesis.

5.1.1. Indicative significance of iron dolomite ring

Because the content of Fe^{2+} is closely related to the CL luminescence intensity of the band [34, 46-47], it is important to analyze the source of Fe^{2+}. There are two sources of Fe in Fengcheng formation iron dolomite: (1) the upwelling of marine brine due to the action of capillary force brought a large amount of Fe. The residual marine brine of the Jiamuhe Formation under the Fengcheng Formation invaded [31], bringing abundant elements such as Fe, Mn, and Mg [58]. (2) Meanwhile, the various microorganisms in the Fengcheng Formation re beneficial for the enrichment of iron elements [17, 20]. (3) Fe elements contributed by medium basic volcanic ash. Volcanic ashes are widely distributed in Fengcheng Formation [31], and medium basic volcanic ashes contain a large amount of Mg, Fe, and other elements [59], which will release a large amount of Fe^{2+} in the process of devitrification of volcanic glasses.

5.1.2. Quartz dissolution

Quartz dissolution is a typical alkaline diagenetic phenomenon [60-61]. Three different quartz dissolution phenomena are found in the core thin sections of Fengcheng Formation: (1) the edge of quartz particles is dissolved, and the edge of the particles is dissolved and becomes serrated or bay shape (Figure 3f); (2) The quartz particles are corroded inside, and microscopic dense "honeycomb" corrosion pits can be seen on the mineral surface in SEM test (Figure 3g); (3) Quartz grains develop irregular linear distribution of fractures, and some of the fractures are locally widened by further corrosion.

The dissolution of quartz in the Fengcheng Formation was affected by Na^+, temperature and alkalinity, and occurred during the burial diagenetic period. Quartz dissolution is closely related to the alkaline diagenetic environment [1, 17, 60, 62], especially with the alkaline cation Na^+, which can form sodium silicate on the surface of quartz particles through hydration reaction, and then crack to cause quartz erosion [63-65]. The Fengcheng Formation rocks were formed in an alkaline lake environment [43-46, 65-66]. The Fengcheng Formation volcanic rocks are sodium-rich volcanic rocks, and the content of Na_2O in the volcanic rocks is much higher than that of K_2O [67], and the Na element mainly exists in albite. The albite content in the volcanic rocks of the Fengcheng Formation is high

 doi:10.20944/preprints202310.1320.v1

[35], and the hydrolysis of albite increases the content of Na+, which causes the cations in the alkaline lake water to be dominated by Na^+ [44]. The alkaline diagenetic environment rich in Na^+ is favorable for quartz dissolution, because the high Na^+ content increases the probability of Na^+ forming complexes on the quartz surface.

Under the same conditions, the dissolution rate of quartz at high temperature (430 °C) is 11 orders of magnitude faster than that at relatively low temperature (25 °C) [68], that is, high temperature is beneficial to the dissolution of quartz. In addition, the pH value also affects the dissolution of quartz. When the predecessors conducted hydrothermal experiments on the dissolution of quartz in an alkaline environment at a temperature of 130 °C and a pH value of 9.5, the quartz was significantly dissolved [61]. Therefore, the ground temperature is calculated according to the burial depth of the Fengcheng Formation, and it is concluded that such temperature conditions can be satisfied [69-70]. The pH value of the alkaline lake during the deposition of the Fengcheng Formation is in the range of 9-11[22]. During the diagenetic stage, the alkalinity decreases, but the temperature increases, the temperature change had a greater impact on the quartz dissolution than the pH change [61]. Therefore, Fengcheng Formation has the condition of quartz dissolution in burial alkaline environment. In addition, due to the quartz dissolution is positively correlated with Na^+, the catalytic activity of the alkaline cation Na^+ increases with the increase of alkalinity [59, 68], and the increase of alkalinity can promote the dissolution of quartz. temperature and alkalinity, the dissolution of quartz is intensified with the rise of temperature in the middle and high-temperature alkaline diagenetic stage. For example, the serrate dissolution of quartz edge is intensified and then becomes harbor, and the local dissolution of internal cracks in quartz minerals is intensified and widened.

5.1.3. Cementation of laumontite

The laumontite in the Fengcheng Formation rocks mostly exists in the state of sheet-like cement (Figure 3h), which is an authigenic aluminosilicate mineral with high content of Ca^{2+}, formed in a neutral-alkaline environment, and the corresponding pH value is mostly 7-10 [71]. The type of zeolite cementation is closely related to the properties of volcanic materials and their hydrolysis [72-73]. As the stratum is buried and the temperature of the stratum rises, a large number of low-temperature unstable minerals contained in the intermediate-basic volcanic rocks (substances) are hydrolyzed to form laumontite cement in an alkaline environment [74]. With the evolution of organic matter in the Fengcheng Formation, a large amount of CO_2 and short-chain organic fatty acids were released [74], and the atmospheric water infiltrated along the Kebai-Wuxia fault belt and the pore water formed by dehydration of clay minerals [75], under the combined action, the early cemented laumontite is dissolutive.

5.1.4. Formation of reedmergnerite

The appearance of reedmergnerite marks the middle-high temperature alkaline diagenesis of the Fengcheng Formation, and its formation is closely related to the hydrothermal fluid. The main evidences are as follows: (1) During the period of the Fengcheng Formation, different rare earth element distributions model shows that the fluids are mainly from endogenous fluids in different parts, including subduction zones, crustal and mantle sources, and the boron required for reedmergnerite may mainly come from deep alkaline hydrothermal fluids[66, 76]; (2) The measurement of boron isotope $\delta^{11}B$ shows that the fluids of different forms of reedmergnerite in the Fengcheng Formation are from the same source, and the fluid may come from deep hydrothermal[66]; (3) Reedmergnerite is widely developed near the fault, and during the Fengcheng Formation, the volcanic activity[31], boron-rich hydrothermal fluids affected by volcanic activity can migrate along developed fault networks; (4) Reedmergnerite is formed in a closed alkaline lake environment [46], and it is not easy for enthetic materials to enter the lake basin through relatively normal and gentle migration, and the hydrothermal fluid in the deep is more capable of entering this closed environment under the external force of the huge energy [66], bringing the required substances; (5) The hydrothermal fluid can provide sufficient reaction temperature, which can reach

 doi:10.20944/preprints202310.1320.v1

the experimental temperature required for the synthesis of reedmergnerite[53-55], while the reedmergnerite in the Fengcheng Formation is developed in the Feng2 with a burial depth greater than 3000 m[66], and in 2018, Rao Song studied the thermal history recovery characteristics of the Junggar Basin by using paleo-temperature scale methods such as vitrinite reflectance and fission track[70], and found that the geothermal gradient of the Fengcheng Formation was 5-3°C/100m. The formation temperature of the reedmergnerite development layer is about 140°C (the average geothermal gradient is 4°C, and the annual average temperature is about 20°C), which cannot reach the temperature threshold required for the formation of reedmergnerite, while the hydrothermal fluid becomes capable of providing the greatest possible chance of such a high temperature.

According to the phenomenon actually observed in the thin slices, it was found that reedmergnerite has a metasomatism relationship with alkaline minerals, such as sodium-calcium carbonate (Figure 3f), trona (Figure 3g), and carbonate minerals (Figure 2h, 3a and 3b). Alkaline minerals and carbonate minerals have certain commonalities. Regarding chemical composition, alkaline minerals are carbonate minerals with different Na^+ contents. Because the composition of carbonate minerals-alkaline minerals is different from that of reedmergnerite, two processes of dissolution and recrystallization are involved in the metasomatism [67]. Different dissolution degrees, different crystal habits and order degrees during recrystallization may be important reasons for the formation of different forms of reedmergnerite [59].

At present, there are different opinions on the division of the formation period of reedmergnerite, including buried diagenetic period and quasi-contemporaneous period [22, 44, 53, 66, 73]. Temperature and pressure are the key factors for the formation of reedmergnerite [73]. The burial is shallow in the quasi-contemporaneous period, the temperature and pressure are not up to the formation conditions of reedmergnerite, and the carbonate minerals and alkaline minerals metasomatized by reedmergnerite are mainly developed in the Feng 2 Member, with burial depth greater than 3000m [66]. Therefore, it is speculated that the reedmergnerite was mainly formed by metasomatism of carbonate minerals and alkaline minerals formed earlier under the action of abnormal hydrothermal during burial diagenesis.

5.2. Diagenetic evolutionary sequence of Fengcheng Formation shale series in Mahu Sag

Characterized by vitrinite reflectance (Ro) of mudstone in Fengcheng Formation and supported by inclusion temperature, most reservoirs in Fengcheng Formation are in middle diagenetic stage A and a small part of them enter middle diagenetic stage B.

5.2.1. Devitrification and hydrolysis

Volcanic glass material is unstable and often altered or devitrified to form stable clay minerals and zeolite under the action of volcanic activities and tectonic movements. Fengcheng Formation contains a large amount of volcanic vitreous originally, which is widely distributed in clastic rock debris and volcanic rock matrix. Influenced by the environment, it can release a large amount of K^+, Na^+, Ca^{2+} and Mg^{2+}, and saline and alkaline interlayer pore water.

5.2.2. Diagenetic mineral precipitation sequence

The first mineral to emerge from the solution is montmorillonite [78]. In the Fengcheng Formation, this part of montmorillonite was gradually transformed to form the Aemon mixed layer. With the further reaction, the salinity and alkalinity of the interlayer solution rose to the range of feldspar precipitation, and the feldspar precipitated was associated with clay minerals, followed by zeolite and quartz precipitation. The early zeolite is unstable, and with a further increase in temperature, it will further generate zeolite and feldspar, and release calcium ions, and the surplus calcium ions promote the formation of calcite [79-80]. Under the conditions of temperature and pressure, and the abundant magnesium and iron ions in the solution, the part of montmorillonite will be transformed into chlorite. Along with the hydrolytic alteration of volcanic glass materials, magnesite minerals such as pyroxene, hornblende, biotite, and feldspar phenocrysts, crystal chips

Preprints (www.preprints.org) | NOT PEER-REVIEWED | Posted: 20 October 2023 doi:10.20944/preprints202310.1320.v1

and potassium feldspar in pyroclastic materials also have some chlorite (Figure. 7). At the same time, the authigenic minerals precipitated under such environmental conditions are as follows: 1. Bicarbonate minerals (carbonaceous calcium stone, trona, carbonaceous sodium magnesite, etc.). 2. Salt minerals (sodium silicate, salt, etc.). 3. Aluminum silicate minerals (potassium feldspar, albite, zeolite, etc.). 4. Calcium and magnesium carbonate minerals (dolomite, calcite, etc.). 5. Siliceous minerals (quartz, opal, etc.) [81].

The alteration process of Fengcheng Formation can be classified as follows: 1. Hydrolysis of volcanic glass -- generation of montmorillonite -- generation of zeolite minerals and related transformation -- albitization; 2. Chlorite influenced by magnesium and iron ions; 3. Feldspar alteration -- formation of chlorite and calcite – rest albite. In particular, hydrolysis occurred in early diagenetic A stage. Dolomite formation can be divided into three stages, most of which are in early diagenetic stage B; Salt minerals are formed in the same generation; There are three phases of dissolution, which are scattered from the late early diagenetic stage to the middle diagenetic stage B (Figure. 7).

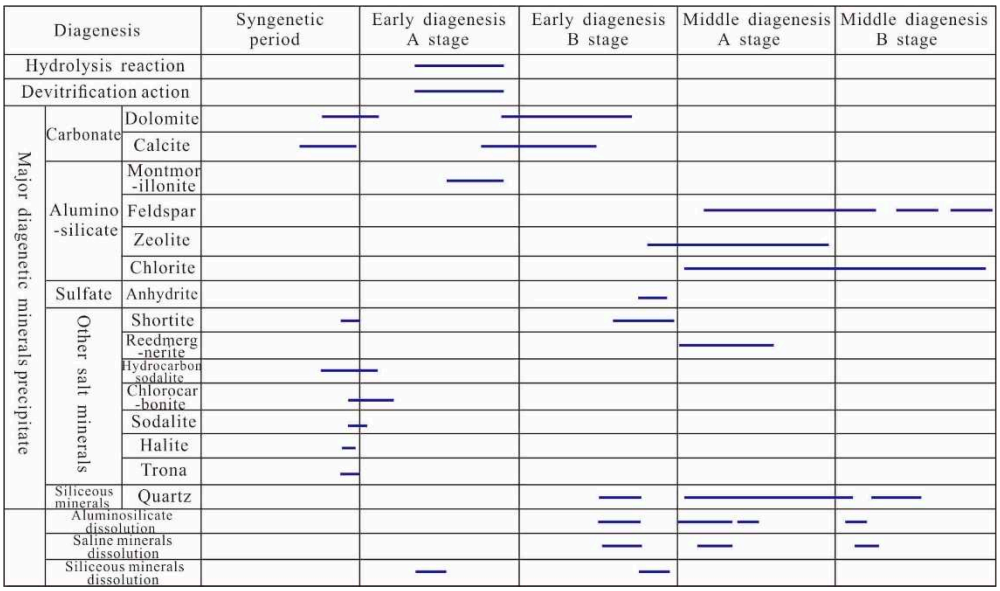

Figure 7. Sequence diagram of diagenetic evolution of Fengcheng Formation in Mahu Sag.

5.3. Alkaline sedimentary evolution and diagenetic model of Fengcheng Formation shale series in Mahu Sag

Based on core slices from wells FN1, FN14, AK-1, and MH7 in the Mahu Sag, combined with literature data, the sedimentary evolution and the diagenetic model of the Fengcheng Formation in the alkaline lake environment were established from the aspects of climate, provenance, diagenetic environment and underground fluids (Figure. 8), which can be roughly divided into four stages: before the deposition of the Fengcheng Formation, during the deposition of the Fengcheng Formation, the low-temperature alkaline burial diagenetic stage, and the hydrothermal-related medium-high temperature alkaline diagenetic stage.

Before the deposition of the Fengcheng Formation, in the arid-semi-arid climate, the lake water evaporated and concentrated [46], resulting in a gradual increase in the alkalinity of the water body [67, 72-73]. In addition, due to active volcanic activity, a large number of volcanic rocks developed at the bottom of the lake basin, and the low-temperature unstable minerals contained in the volcanic rocks were hydrolyzed, which provided Na^{+}, Ca^{2+}, Mg^{2+}, and Fe^{2+} for the water body, which laid the material foundation for diagenesis and alkaline lake formation (Figure 8a).

Preprints (www.preprints.org) | NOT PEER-REVIEWED | Posted: 20 October 2023 doi:10.20944/preprints202310.1320.v1

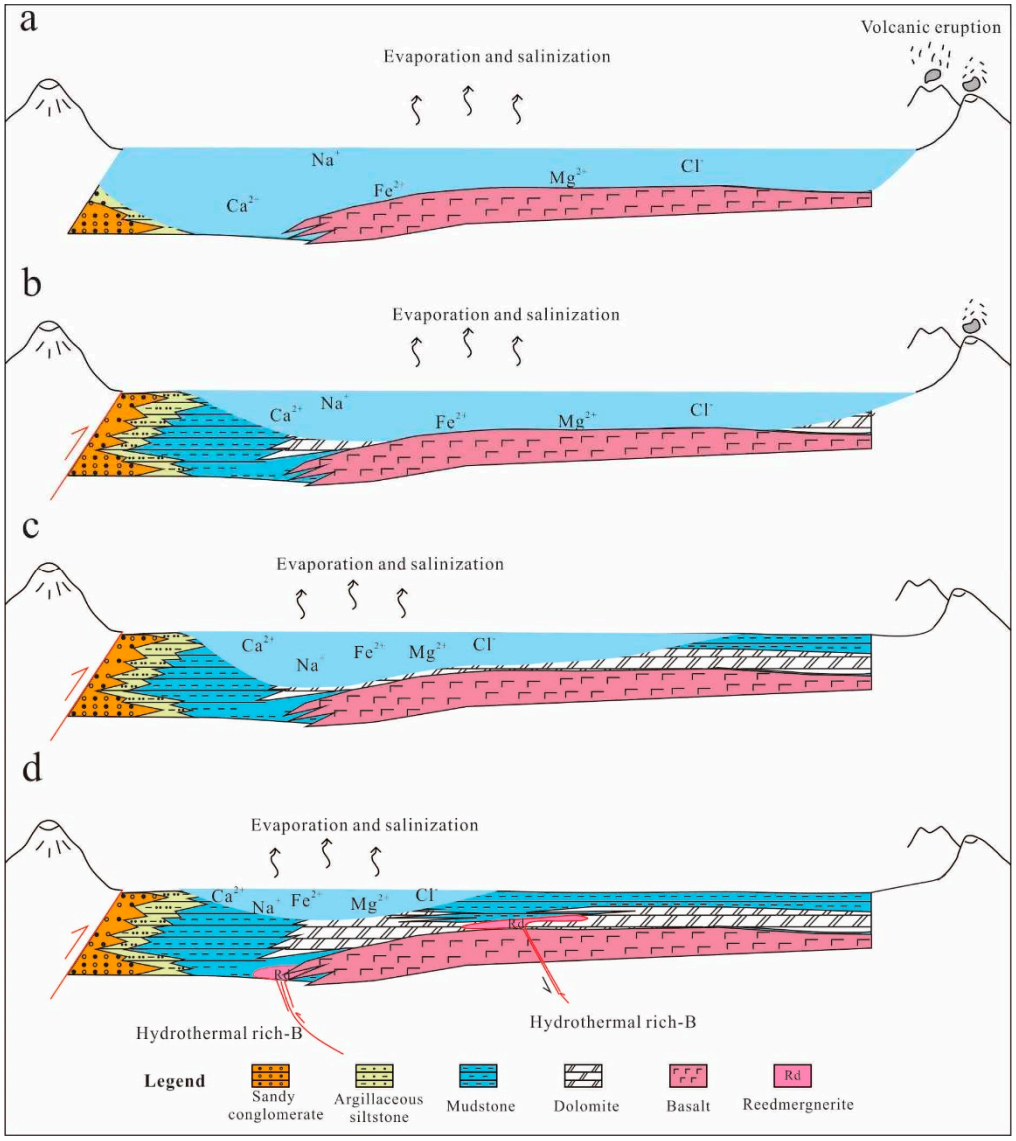

Figure 8. Alkaline sedimentary evolution-diagenesis model of the Fengcheng Formation (The faults shown are schematic faults.

During the deposition of the Fengcheng Formation, there were Cl^-, CO_3^{2-}, SO_4^{2-}, and other anions in the lake basin. During the process of lake basin shrinkage and alkalization, the concentration of ions gradually increased, collided and combined with each other, and a large number of Mg-Ca carbonate minerals and alkaline minerals with anions of CO_3^{2-} appeared. In the presence of Mg^{2+}, Na^+, and Ca^{2+} plasmas, the order of binding with HCO_3^- and CO_3^{2-} is Ca^{2+}, Mg^{2+}, Na^+ [58], $CaCO_3$ precipitation before $MgCO_3$, after calcite precipitation, the lake water is stratified under the action of evaporation and concentration, which promotes the development of argillaceous sediments rich in organic matter [27]. The types of organic matter are mainly from that organic matter [82-83], and their decay products are conducive to the large-scale development of carbonate minerals, forming lamellar carbonate mineral layers (mainly calcite) and argillaceous sediment layers. At this time, due to the large consumption of Ca^{2+}, the Mg^{2+}/Ca^{2+} ratio in the water body increases, and the Fe^{2+} contributed by the volcanic tuff material, the microcrystal dolomite deposited[84]. The extensive development of carbonate minerals consumes a large amount of Ca^{2+} and Mg^{2+}, while the content of Na^+ increases relatively, and the consumed CO_3^{2-} is continuously supplemented by volcanic activity.

With the further shrinkage of the lake basin water body, the alkalinity reaches the maximum, Na^+ and CO_3^{2-} tend to be saturated, and Na^+ containing alkaline minerals such as trona and sodium-calcium carbonate are formed successively. Finally, the climate became hot and humid, and the water

 doi:10.20944/preprints202310.1320.v1

level rise, under the supply of terrigenous detrital materials, terrigenous detrital materials such as mud and sand were deposited, and the sedimentary strata of the Fengcheng Formation were deposited (Figure 8b).

In the low-temperature alkaline diagenetic stage, the residual marine brine in the Carboniferous and Jiamuhe Formations underlying the Fengcheng Formation from the mid-Permian to the mid-Jurassic [31], entering into the pores and fractures of the Fengcheng Formation along the fault under tectonic compression, it brought abundant elements such as Fe, Mn and Mg [58], and cemented around the early calcite or calcite with a low degree of dolomitization, the local distribution of fine-grained iron dolomite with clear ring is formed. With the surging of residual marine brine, Na^+ is also present. In addition, the two necessary conditions of alkaline formation water and the rising temperature due to the formation's burial are also present. The dissolution of quartz occurs, the "salt effect" of Mg^{2+}, K^+ and Ca^{2+} in formation water will further promote the dissolution of quartz [62]. In this stage, in addition to the formation of iron dolomite and quartz dissolution, the cementation of laumontite also occurred under the background of alkaline diagenesis, low temperature and the supply of Mg^{2+} and Fe^{2+} (Figure 8c).

The hydrocarbon source rocks of the Fengcheng Formation did not enter the oil generation threshold until the end of the Permian period [85], and kerogen began to transform into oil and gas. This process was accompanied by the formation of oxalic acid and acetic acid [13], where local pore fluid pH drops and becomes acidic, resulting in the dissolution of early turbidite, iron dolomite and alkaline minerals. The acidic fluid generated by oil and gas is neutralized by alkaline formation water and alkaline minerals, and the whole presents an alkaline diagenetic environment. During the middle-high temperature alkaline diagenesis stage, the hydrothermal activity was intense at the end of the Triassic [74], and the B-rich hydrothermal fluid migrated and upwelled along the fault. Reedmergnerite is formed by alkaline minerals containing Na^+. Correspondingly, the mineral assemblages of reedmergnerite + calcite + iron dolomite, reedmergnerite + shortite and reedmergnerite + mineral assemblages of trona can be found in the parts with incomplete metasomatism. Under the influence of the intercalated horizon of the fault, the distribution and morphology of the metasomatic minerals and other factors, banded and agglomerated reedmergnerite are formed. As the overlying material continues to deposit, the burial depth increases. When the stone is enriched to a certain extent, it forms reedmergnerite-rich rocks (Figure 8d). Marked by the appearance of reedmergnerite, medium-high temperature alkaline diagenesis occurred in the center and slope of the Mahu sag and near the fault zone connecting the deep fluid and alkaline mineral layer-carbonate layer [66].

6. Conclusions

In this paper, the types of shale series developed in the Fengcheng Formation in the Mahu Sag include carbonate rocks, terrigenous detrital rocks and alkaline mesobasic volcanic rocks, and there are bands and agglomerates rich in reedmergnerite. Under the combined influence of the supply of sodium-rich sources, an alkaline lake characterized by the development of alkaline minerals was formed, and experienced alkaline deposition and diagenesis in an alkaline environment.

There are 3 types of diagenetic mineral assemblages and 2 types of alkaline diagenesis developed in the shale series of the Fengcheng Formation. 3 mineral combinations include: carbonate mineral combination (calcite + iron dolomite), reedmergnerite and carbonate mineral combination (reedmergnerite + calcite + iron dolomite) and reedmergnerite and alkaline minerals combination (reedmergnerite + shortite + trona). According to the diagenetic temperature, the alkaline diagenesis of the Fengcheng Formation can be divided into two types: low-temperature alkaline burial diagenesis and medium-high-temperature alkaline diagenesis. The former is characterized by the formation of iron dolomite rings, the dissolution of quartz and the cementation of laumontite, while the latter is characterized by the abundant appearance of reedmergnerite.

Under the promotion of a long-term arid-semi-arid climate, based on underground fluids (hydrothermal and brine) and alkaline medium-basic volcanic parent rocks (substances) as the main material sources, in the special alkaline diagenetic environment of alkali lake, the alkaline

sedimentary evolution-diagenetic model of the Fengcheng Formation, which is affected by climate, provenance, diagenetic environment, and underground fluid, has been established. The model is divided into four stages: before the deposition of the Fengcheng Formation, sedimentary, low-temperature alkaline burial diagenesis and hydrothermally related medium-high temperature alkaline diagenesis.

Author Contributions: Conceptualization, methodology and writing, B.B. and J.L.; review and editing, Z.Y.; validation, Y.B. and X.C.; analysis and investigation, M.Z. and H.L.; supervision and editing, H.Z. All authors have read and agreed to the published version of the manuscript.

Funding: National Natural Science Foundation of China (No. 52004232, U19A200380), Sichuan Province Science and Technology Support Program (23QYCX0060, JG2021-624, 2021YFS0305, 22YFQ0061) and Sichuan Provincial Key Lab of Process Equipment and Control (GK202006).

Institutional Review Board Statement: Not applicable.

Data Availability Statement: There is no associate data in this study.

Conflicts of Interest: The authors declare no conflict of interest.

Abbreviations

The following abbreviations are used in this manuscript:

EPMA	electron probe microanalysis
SEM	scanning electron microscope
CL	cathode luminescence
LR	laser Raman
Cal	calcite
Fer-DOL	ferric dolomite
Rd	reedmergnerite
Tro	trona
St	shortite
Lmt	Laumonite cemented between particles

References

1. Kuang, L. C.; Tang, Y.; Lei, D. W.; Chang, Q. S.; Ouyang, M.; Hou, L. H.; Liu, D. G. Formation conditions and exploration potential of tight oil in the Permian saline lacustrine dolomitic rock, Junggar Basin, NW China. Petroleum Exploration and Development. 2012. 39, 657-667.
2. Kuang, L. C.; Cui, X. K.; Zou, C. N.; Hou, L. H. Oil accumulation and concentration regularity of volcanic lithostratigraphic oil reservoir: A case from upper-plate Carboniferous of KA-BAI fracture zone, Junggar Basin. Petroleum Exploration and Development. 2007. 34, 285-290.
3. Yu, K.; Cao, Y.; Qiu, L.; Sun, P. The hydrocarbon generation potential and migration in an alkaline evaporate basin: The Early Permian Fengcheng Formation in the Junggar Basin, northwestern China. Marine and Petroleum Geology. 2018. 98, 12-32.
4. Jagniecki, E. A.; Jenkins, D. M.; Lowenstein, T. K.; Carroll, A. R. Experimental Study of Shortite (Na2Ca2(CO3)3) Formation and Application to the Burial History of the Wilkins Peak Member, Green River Basin, Wyoming, USA. Geochimica et Cosmochimica Acta. 2013. 115, 31-45.
5. Smith, M. E.; Carroll, A. R.; Singe, B. S. Synoptic Reconstruction of a Major Ancient Lake System:Eocene Green River Formation, Western United States. Geological Society of America Bulletin. 2008. 1-2, 54-84.
6. Javier, G. V.; Ibrahim, G.; Cahit, H.; Eva, P. Genetic Model for Na-Carbonate Mineral Precipitation in the Miocene Beypazarı Trona Deposit, Ankara Province, Turkey. Sedimentary Geology. 2013. 294, 315-327.
7. Meng, T.; Liu, P.; Qiu, L. W.; Wang, Y. S.; Liu, Y. L.; Lin, H. M.; Cheng, F. Q.; Qu, C. S. Formation and distribution of the high quality reservoirs in a deep saline lacustrine basin: A case study from the upper part of the 4th member of Paleogene Shahejie Formation in Bonan sag, Jiyang depression, Bohai Bay Basin, East China. Petroleum Exploration and Development. 2017. 44, 896-906.
8. Tang, Y.; Lyu, Z. X.; He, W. J.; Qing, Y. H.; Li, X.; Song, X. Z.; Yang, S.; Cao, Q. M.; Qian, Y. X.; Zhao, X. M. Origin of dolomites in the Permian dolomitic reservoirs of Fengcheng Formation in Mahu Sag, Junggar Basin, NW China. Petroleum Exploration and Development. 2023. 50, 38-50.
9. Jiang, F. J.; Hu, M. L.; Hu, T.; Lyu, J. H.; Huang, L. L.; Liu, C. L.; Jiang, Z. X.; Huang, R. D.; Zhang, C. X.; Wu, G. Y.; Wu, Y. P. Controlling factors and models of shale oil enrichment in Lower Permian Fengcheng

Formation, Mahu Sag, Junggar Basin, NW China. Petroleum Exploration and Development. 2023. 50, 706-718.
10. Tang, Y.; Cao, J.; He, W. J.; Guo, X. G.; Zhao, K. B.; Li, W. W. Discovery of shale oil in alkaline lacustrine basins: The Late Paleozoic Fengcheng Formation, Mahu Sag, Junggar Basin, China. Petroleum Science. 2021. 18, 1281-1293.
11. Qiu, L.W.; Jang, Z.X.; Cao, Y.C.; Qiu, R.H.; CHEN, W.X.; TU, Y.F. Alkaline diagenesis and its influence on a reservoir in the Biyang depression. *Science in China (Series D)*. **2002**, *45*, 643-653.
12. Li, S.Y.; Tian, J.C.; Lin, X.B.; Zuo, Y.H.; Kang, H.; Yang, D.D. Effect of alkaline diagenesis on sandstone reservoir quality: Insights from the Lower Cretaceous Erlian Basin, China. *Energy Exploration & Exploitation*. **2002**, *38*, 434-453.
13. Zhang, S.B.; Liu, Z.; Liu, H.J.; Song, Y.H.; Li, X.M.; Xu, T. Alkali Diagenesis of Xujiahe Sandstone in Hebaochang Block in Sichuan Basin. *Xingjiang Petroleum Geology*. **2011**, *32*, 464-468.
14. Cao, T.Y.; Zhong, D.K.; Niu, S.L.; Sun, H.T.; Cao, X.; Wang, F. Alkaline Diagenesis and Porosity Evolution of Zhu hai Formation Reservoirs in Eastern Huizhou Sag. *Acta Sedimentologica Sinica*. **2020**, *38*, 1327-1337.
15. Zhu, H.H.; Zhong, D.K.; Yao, J.L.; Sun, H.T.; Niu, X.B.; Liang, X.W.; You, Y.; Li, X. Alkaline diagenecs and its effects on reservoir porosity: A case study of Upper Triassic Chang 7 Member tight sandstone in Ordos Basin, NW China. *Petroleum Exploration and Development*. **2015**, *42*, 56-65.
16. Hu, T.; Pang, X.Q.; Jiang, S.; Wang, Q.F.; Xu, T.W.; Lu, K.; Huang, C.; Chen, Y.Y.; Zheng, X.W. Impact of Paleosalinity, Dilution, Redox, and Paleoproductivity on Organic Matter Enrichment in a Saline Lacustrine Rift Basin: A Case Study of Paleogene Organic-Rich Shale in Dongpu Depression, Bohai Bay Basin, Eastern China. *Energy & Fuels*. **2008**, *32*, 5045-5061.
17. Chen, Z.Y.; Chen, J.F.; Zhong, N.N.; Fei, W.W.; Dong, Q.W.; Chen, J.; Wang, Y.Y. The geneses of sedimentary organic matter with anomalous 13C-enriched isotopic composition in saline and freshwater lakes: A case study of lacustrine source rocks from Dongpu and Qikou sags, Bohai Bay Basin, eastern China. *Marine and Petroleum Geology*. **2020**, *118*, 104434.
18. Wang, K.; Pang, X.Q.; Zhang, H.G.; Zhao, Z.F.; Su, S.C.; Hui, S.S. Characteristics and genetic types of natural gas in the northern Dongpu Depression, Bohai Bay Basin, China. *Journal of Petroleum Science and Engineering*. **2018**, *170*, 453-466.
19. Tan, X.F.; Tian, J.C.; Li, Z.B.; Zhang, S.P.; Wang, W.Q. Diagenesis evolution of fragmental reservoir in alkali sediment environment-taking the Member 4 of Shahejie Formation of steep-slope zone in Dongying sag, Shandong, China for example. *Geological Bulletin of China*. **2010**, *4*, 535-543.
20. Cao, J.; Lei, D.W.; Li, Y.W.; Tang, Y.; Abulimiti.; Chang, Q.S.; Wang, T.T. Ancient high-quality alkaline lacustrine source rocks discovered in the Lower Permian Fengcheng Formation, Junggar Basin. *Acta Petrolei Sinica*. **2015**, *36*, 781-790.
21. Cao, J.; Xia, L.W.; Wang, T.T.; Zhi, D.M. An alkaline lake in the Late Paleozoic Ice Age (LPIA): A review and new insights into paleoenvironment and petroleum geology. *Earth-Science Reviews*. **2020**, *202*, 103091.
22. Zhang, Z.J.; Yuan, X.J.; Wang, M.S.; Zhou, C.M.; Tang, Y.; Chen, X.Y.; Lin M.J.; Cheng, D.W. Alkaline-lacustrine deposition and paleoenvironmental evolution in permian fengcheng formation at the mahu sag, junggar basin, nw china. *Petroleum Exploration and Developmen*t. **2018**, *45*, 1036-1049.
23. Yu, K.H.; Cao, Y.C., Qiu, L.W., Sun, P.P.; Jia, X.Y.; Wan, M. Geochemical characteristics and origin of sodium carbonates in a closed alkaline basin: The Lower Permian Fengcheng Formation in the Mahu Sag, northwestern Junggar Basin, China. *Palaeogeography, Palaeoclimatology, Palaeoecology*. **2018**, *511*, 506-531.
24. Tang, W.B.; Zhang, Y.Y.; Georgia, P.P.; David, J.W.P.; Guo, Z.J.; Li, W. Permian to early Triassic tectono-sedimentary evolution of the Mahu sag, Junggar Basin, western China: sedimentological implications of the transition from rifting to tectonic inversion. *Marine and Petroleum Geology*. **2021**, *123*, 104730.
25. He, D.F.; Li, D.; Fan, C.; Yang, X.F. Geochronology, geochemistry and tectonostratigraphy of Carboniferous strata of the deepest Well Moshen-1 in the Junggar Basin, northwest China: Insights into the continental growth of Central Asia. *Gondwana Research*. **2013**, *24*, 560-577
26. He, D.F.; Zhang, L.; Wu, S.T.; Li, D.; Zhen, Y. Tectonic evolution stages and features of the Junggar Basin. *Oil & Gas Geology*. **2018**, *39*, 845-861.
27. He, D.F.; Yin, C.; Du, S.K.; Shi, X.; Ma, H.S. Characteristics of structural segmentation of foreland thrust belts -A case study of the fault belts in the northwestern margin of Junggar Basin. *Earth Science Frontiers*. **2004**, *3*, 91-101.
28. Cao, J.; Yao, S.P.; Jin, Z.J.; Hu, W.X.; Zhang, Y.J.; Wang, X.L.; Zhang, Y.Q.; Tang, Y. Petroleum migration and mixing in the northwestern Junggar Basin (NW China): constraints from oil-bearing fluid inclusion analyses. *Organic Geochemistry*. **2006**, *37*, 827-846.
29. Xu, Z.H.; Hu, S.Y.; Wang, L.; Zhao, W.Z.; Cao, Z.L.; Wang, R.J.; Shi, S.Y.; Jiang, L. Seismic sedimentologic study of facies and reservoir in middle Triassic Karamay Formation of the Mahu Sag, Junggar Basin, China. *Marine and Petroleum Geology*. **2019**, *107*, 222-236.

30. Li, D.; He, D.F.; Santosh, M.; Ma, D.L.; Tang, J.Y. Tectonic framework of the northern Junggar Basin part I: The eastern Luliang Uplift and its link with the East Junggar terrane. *Gondwana Research*. **2015**, *27*, 1089-1109.
31. Zhu, S.F.; Zhu, X.M.; Niu, H.P.; Han, X.F.; Zhang, Y.Q. Genetic Mechanism of Dolomitization in Fengcheng Formation in the Wu-Xia area of Junggar Basin, China. *Acta Geologica Sinica-english Edition*. **2012**, *86*, 447-461.
32. Hou, L.H.; Zou, C.N.; Liu, L.; Wen, B.H.; Wu, X.Z.; Wei, Y.Z.; Mao, Z.G. Geologic essential elements for hydrocarbon accumulation with in Carboniferous volcanic weathered crusts in Xinjiang, China. *Acta Petrolei Sinica*. **2012**, *33*, 533-540.
33. Wu, W.; Li, Q.; Pei, J.X.; Ning, S.Y.; Tong, L.Q.; Liu, W.Q.; Feng, Z.D. Seismic sedimentology, facies analyses, and high-quality reservoir predictions in fan deltas: A case study of the Triassic Baikouquan Formation on the western slope of the Mahu Sag in China's Junggar Basin. *Marine and Petroleum Geology*. **2020**, *120*, 104546.
34. Chen, Z.L.; Liu, G.D.; Wang, X.L.; Gao, G.; Xiang, B.L.; Ren, J.L.; Ma, W.Y.; Zhang, Q. Origin and mixing of crude oils in Triassic reservoirs of Mahu slope area in Junggar Basin, NW China: Implication for control on oil distribution in basin having multiple source rocks. *Marine and Petroleum Geology*. **2016**, *78*, 373-389.
35. Liang, Y.Y.; Zhang, Y.Y.; Chen, S.; Guo, Z.J.; Tang. W.B. Controls of a strike-slip fault system on the tectonic inversion of the Mahu depression at the northwestern margin of the Junggar Basin, NW China. *Journal of Asian Earth Sciences*. **2020**, *198*, 104229.
36. Lei, W.D.; Chen, G.Q.; Liu, H.L.; Li, X.; Abulimiti.; Tao, K.Y.; Cao, J. Study on the forming conditions and exploration fields of the Mahu Giant Oil (Gas) Province, Junggar Basin. *Acta Geologic Sinica*. **2017**, *91*, 1604-1619.
37. Zhang, G.Y.; Wang, Z.Z.; Guo, X.G.; Sun, Y.Y.; Sun, L.; Pan, L. Characteristics of lacustrine dolomitic rock reservoir and accumulation of tight oil in the Permian Fengcheng Formation, the western slope of the Mahu Sag, Junggar Basin, NW China. *Journal of Asian Earth Sciences*. **2019**, *178*, 64-80.
38. Chen, Y.B.; Cheng, X.G.; Zhang H.; Li, C.Y.; Ma, Y.P.; Wang, G.D. Fault characteristics and control on hydrocarbon accumulation of middle-shallow layers in the slope zone of Mahu sag, Junggar Basin, NW China. *Petroleum Exploration and Development*. **2018**, *6*, 1050-1060.
39. Feng, C.; Li T.; He, W.J.; Zheng, M.L. Organic geochemical traits and paleo-depositional conditions of source rocks from the Carboniferous to Permian sediments of the northern Mahu Sag, Junggar Basin, China. *Journal of Petroleum Science and Engineering*. **2020**, *191*, 107117.
40. Li, J.; Tang, Y.; Wu, Tao.; Zhao, J.Z.; Wu, H.Y.; Wu, W.T.; Bai, Y.B. Overpressure origin and its effects on petroleum accumulation in the conglomerate oil province in Mahu Sag, Junggar Basin, NW China. *Petroleum Exploration and Development*. **2020**, *47*, 726-739.
41. Yang, M.Z.; Wang, F.Z.; Zheng, J.P. Geochemistry and tectonic setting of basic volcanic rocks in Ke-Xia region, northwestern Junggar Basin. *Acta Petrologica Et Mineralogica*. **2006**, *20*, 165-174.
42. Chang, L.H.; Chen, M.Y.; Jin, W.; Li, S.C.; Yu, J.J. *Handbook of Identification of transparent mineral slices*. 1st ed.; Geological Publishing House, Beijing, China, **2006**; pp. 1-259.
43. Jiang, Y.Q.; Wen, H.G.; Qi, L.Q.; Zhang, X.X.; Li, Y. Salt minerals and their genesis of the permian Fengcheng Formation in urho area, Junggar Basin. *Mineralogy and Petrology*. **2012**, *32*, 105-114, 2012.
44. Wang, M.S.; Zhang, Z.J.; Zhou, C.M.; Yuan, X.J.; Lin, M.J.; Liu, Y.H.; Cheng, D.W. Lithological characteristics and origin of alkaline lacustrine of the Lower Permian Fengcheng Formation in Mahu Sag, Junggar Basin. *Journal of Paleogeography*. **2018**, *20*, 147-162.
45. Xu, L.; Chang, Q.S.; Feng, L.L.; Zhang, N.; Liu, H. The reservoir characteristics and control factors of shale oil in Permian Fengcheng Formation of Mahu sag, Junggar Basin. *China Petroleum Exploration*. **2019**, *24*, 649-660.
46. Yu, K.H.; Cao, Y.C.; Qiu, L.W.; Sun, P.; Yang, Y.Q.; Qu, C.S.; Wan, M. Characteristics of alkaline layer cycles and origin of the Lower Permian Fengcheng Formation in Mahu sag, Junggar Basin. *Journal of Paleogeography*. **2016**, *18*, 1012-1029.
47. You, X.L.; Jia, W.Q., Xu, F.; Liu, Y. Mineralogical characteristics of ankerite and mechanisms of primary and secondary origins. *Earth Science*. **2018**, *43*, 4046-4055.
48. Pagel, M.; Barbin, V.; Blanc, P.; Ohnenstetter, D. *Application of Cathodoluminescence to Carbonate Diagenesis*. 1st ed.; Springer-Verlag, Berlin, Germary, **2000**; pp. 271-301.
49. Ma, P.J.; Lin, C.Y.; Jahren, J.; Dong, C.M.; Ren, L.H.; Hellevang, H. Cyclic zoning in authigenic saddle dolomite-ankerite: Indications of a complex interplay between fault-rupturing and diagenetic alteration. *Chemical Geology*. **2021**, *559*, 119831.
50. Qin, Y.J.; Feng, Y.C.; Yang, X.; Wen, L.Y. A microarea analysis technique of EPMA to probe reedmergnerite. *Journal of Chinese Electron Microscopy Society*. **2016**, *35*, 217-222.
51. Axel, G.; Detlev, K.R; Jan, M.; Rolf, D.N.; Andreas, S. Quantitative high resolution cathodoluminescence spectroscopy of diagenetic and hydrothermal dolomites. *Sedimentary Geology*. **2001**, *140*, 191-199.
52. Braith, J.R. Cathodoluminescence in Quaternary caibonate deposits. *Sedimentary Geology*. **2016**, *337*, 29-35.
53. Goldstein H R. Systematics of fluid inclusions in diagenetic minerals. *SEPM short course*, **1994**, 31, 199.

54. Eugster, H.P.; Mciver, N.L. Boron analogues of alkali feldspars and related silicates. *Bulletin of the Geological Society of America*. **1959**, *70*, 1598.
55. Mitsuyoshi, K. Synthesis and properties of reedmergnerite. *The Journal of the Japanese Association of Mineralogists, Petrologists and Economic Geologists*. **1977**, *72*, 162-172.
56. Liu, L.H.; Huang, S.J.; Wang, C.L.; Huang, K.K.; Tong, H.P.; Zhong, Q.Q. Cathodoluminescence zonal texture of calcite cement in carbonate rock and its relationship with trace element composition:a case of Ordovician carbonate rock of Tahe oilfield, Tarim basin. *Marine Origin Petroleum Geology*. **2010**, *15*, 55-60.
57. Richter, D.K.; Goette, T.; Niggemann, S.; Wurth, G. REE^{3+} and Mn^{2+} activated cathodoluminescence in lateglacial and holocene stalagmites of central europe: evidence for climatic processes? *Holocene*. **2004**, *14*, 759-768.
58. Lovley, D.R.; Holmes, D.E.; Nevin, K.P. Dissimilatory Fe(III) and Mn(IV) reduction. *Advances in Microbial Physiology*. **2004**, *49*, 219-286.
59. Xue, J.J.; Sun, J.; Zhu, X.M.; Liu, W.; Zhu, S.F. Characteristics and Formation Mechanism for Dolomite Reservoir of Permian Fengcheng Formation in Junggar Basin. *Geoscience*. **2012**, *26*, 755-761.
60. Qiu, L.W.; Jiang, Z.X.; Chen, W.X. A new type of secondary porosity--quartz dissolution porosity. *Acta Sedimentologica Sinica*. **2002**, *4*, 621-627.
61. Qu, X.Y.; Chen, X.; Qiu, L.W.; Zhang, M.L.; Zhang, X.J. Genesis of secondary pore of quartz dissolution type and its influences on reservoir: Taking the tight sandstone reservoir in the Upper Paleozoic of Daniudi gas field as an example. *Oil & Gas Geology*. **2015**, *36*, 804-813.
62. Liu, J.K.; Peng, J.; Shi, Y.; Bao, Z.F.; Sun, Y.L.; Liu, X.M.; Zhang, Z. The genesis of quartz dissolution in tight sand reservoirs and its impact on pore development: a case study of Xujiahe Formation in the transitional zone of Central-Southern Basin. *Acta Petrolei Sinica*. **2015**. *36*, 1090-1097.
63. Rimstidt, J.D.; Zhang, Y.L.; Zhu, C. Rate equations for sodium catalyzed amorphous silica dissolution. *Geochimica Et Cosmochimica Acta*. **2016**. *195*, 120-125.
64. Zhang, S.T.; Liu, Y. Molecular-level mechanisms of quartz dissolution under neutral and alkaline conditions in the presence of electrolytes. *Geochemical Journal*. **2014**. *48*, 189-205.
65. Yu, K.H.; Cao, Y.C.; Qiu, L.W.; Sun, P.P. ; Su, Y.G. Brine evolution of ancient lake and mechanism of carbonate minerals during the sedimentation of Early Permian Fengcheng Formation in Mahu Depression, Junggar Basin, China. *Natural Gas Geoscience*. **2016**. *27*, 1248-1263.
66. Zhao, Y.; Guo, P.; Lu, Z.Y.; Zheng, R.C.; Chang, H.L.; Wang, G.Z.; Wei, Y.; Wen, H.G. Genesis of Reedmergnerite in the Lower Permian Fengcheng Formation of the Junggar Basin, NE China. *Acta Sedimentologica Sinica*. **2020**. *38*, 966-979.
67. Zhang, H.; Cheng, L.; Fan, H.T. Formation overpressure and its influence on physical properties in Mahu sag, Junggar Basin. *Progress in Geophysics*. **2021**. 1-8.
68. Zhang, S.T.; Liu, Y. Progress Review of Quartz Dissolution Models. *Bulletin of Mineralogy, Petrology and Geochemistry*. **2009**. *28*, 294-300.
69. Tian, X.R.; Zhang, Y.Y.; Zhuo, Q.G.; Yu, Z.C.; Guo, Z.J. Tight oil charging characteristics of the Lower Permian Fengcheng Formation in Mahu sag, Junggar Basin: evidence from fluid in alkaline minerals. *Acta Petrolei Sinica*. **2019**. *40*, 646-659.
70. Rao, S.; Zhu, Y.K.; Hu, S.B.; Wang, Q. The Thermal History of Junggar Basin: Constraints on the Tectonic Attribute of the Early-Middle Permian Basin. *Acta Geologica Sinica*. **2018**. *92*, 1176-1195.
71. Zhu, S.F.; Zhu, X.M.; Wu, D.; Liu, Y.H.; Li, P.P.; Jiang, S.X.; Liu, X.C. Alteration of volcanics and its controlling factors in the Lower Permian reservoirs at northwestern margin of Junggar Basin. *Oil & Gas Geology*. **2014**. *35*, 77-85.
72. Guo, M.Z.; Shou. J.F.; Xu, Y.; Guo, H.J.; Zou, Z.W. Han, S.H. Distribution and controlling factors of Permian zeolite cements in Zhongguai—Northwest margin of Junggar Basin. *Acta Petrolei Sinica*. **2016**. *37*, 695-705.
73. Chipera, S.J.; Goff, F.; Goff, C.J.; Fittipaldo, M. Zeolitization of intracaldera sediments and rhyolitic rocks in the 1.25 Ma lake of Valles caldera, New Mexico, USA. *Journal of Volcanology & Geothermal Research*. **2008**. *178*, 317-330.
74. Zhu, S.F.; Zhu, X.M. Liu, X.C.; Li, C.; Wang, X.X.; Tan, M.X.; Geng, M.Y.; Li, Y.P. Alteration products of volcanic materials and their influence on reservoir space in hydrocarbon reservoirs: evidence from Lower Permian strata in Ke-Xia region, Junggar Basin. *Acta Petrolei Sinica*. **2014**. *35*, 276-285.
75. Zhu, S.F.; Zhu, X.M.; Wang, X.L.; Liu, Z.Y. Zeolite diagenesis and its control on petroleum reservoir quality of Permian in northwestern margin of Junggar Basin, China. *Science China Earth Sciences*. **2012**. *55*, 386-396.
76. Chang, H.L.; Zheng, R.C.; Guo. C.L.; Wen, H.G. Characteristics of Rare Earth Elements of Exhalative Rock in Fengcheng Formation, Northwestern Margin of Jungger Basin. *Geological Review*, **2016**. *62*, 550-568.
77. Jia, B.; Wen, H.G.; Li, Y.B.; Liu, Y.P.; Wang, T. Fluid inclusions in the salt minerals from the Permian Fengcheng Formation in the Urho region, Junggar Basin, Xinjiang. *Sedimentary Geology and Tethyan Geology*. **2015**. *35*, 33-42.
78. Broxton, D.E. Chemical changes associated with zeolitization of the tuffaceous beds of Calico Hills, Yucca Mountain, Nevada, USA. *Proceedings - International Symposium on Water-Rock Interaction*. **1992**. *7*, 699-703.

79. Lijima, A. Zeolites in petroleum and natural gas reservoirs. *Reviews in Mineralogy and Geochemistry*. **2001**. *45*, 347-402.
80. Zhu, S.F.; Zhu, X.M.; Wu, D.; Liu, Y. Volcanic material alteration and its controlling factors in Lower Permian oil and gas reservoirs in the northwestern margin of Junggar Basin. *Oil & Gas Geology*. **2014**. *35*, 77-85.
81. Zhu, S.F.; Zhu, X.M.; Liu,Y.H.; Chen, X.Y.; Wang, J.H.; Wang, X.J.; Ma, A.Y. Petrological and Geochemical Features of Dolomitic Rocks in the Lower Permian Fengcheng Formation in Wuerhe-Xiazijie Area, Junggar Basin. *Geological Review*. **2014**. *60*, 1113-1122.
82. Jin, Q.; Wang, J.; Song, G.Q.; Wang, L.; Lin, L.M.; Bai, S.P. Interaction between source rock and evaporite: a case study of natural gas generation in the northern dongying depression. *Chinese Journal of Geochemistry*. **2010**. *29*, 75-81.
83. Zhi, D.M.; Tang, Y.; Zheng, M.L.; Xu, Y.; Cao, J.; Ding, J.; Zhao, C.Y. Geological characteristics and accumulation controlling factors of shale reservoirs in Fengcheng Formation, Mahu sag, Junggar Basin. *China Petroleum Exploration*. **2019**. *24*, 615-623.
84. Hips, K.; Haas, J.; Poros, Z.; Kele, S.; Budai, T. Dolomitization of Triassic microbial mat deposits (Hungary): Origin of microcrystalline dolomite. *Sedimentary Geology.* **2015.**318,113-129.
85. Cao, J.; Zhang, Y.J.; Hu, W.X.; Yao, S.P.; Wang, X.L.; Zhang, Y.Q.; Tang, Y. The Permian hybrid petroleum system in the northwest margin of the Junggar Basin, northwest China. *Marine and Petroleum Geology*. **2005**. *22*, 331-349.